Published in final edited form as:

J Exp Zool A Ecol Integr Physiol. 2020 August ; 333(7): 511–525. doi:10.1002/jez.2393.

IS AQUAPORIN-3 INVOLVED IN WATER-PERMEABILITY CHANGES IN THE KILLIFISH DURING HYPOXIA AND NORMOXIC RECOVERY IN FRESHWATER OR SEAWATER?

Ilan M. Ruhr[1,2], **Chris M. Wood**[1,3,4,*], **Kevin L. Schauer**[1], **Yadong Wang**[1], **Edward M. Mager**[1,5], **Bruce Stanton**[6], **Martin Grosell**[1]

[1]Department of Marine Biology and Ecology, Rosenstiel School of Marine and Atmospheric Science, University of Miami, Miami, FL, USA;

[2]Present Address: Cardiovascular Sciences, School of Medical Sciences, University of Manchester, Manchester, UK;

[3]Department of Zoology, University of British Columbia, Vancouver, Canada;

[4]Department of Biology, McMaster University, Hamilton, Canada;

[5]Present Address: Department of Biological Sciences, Advanced Environmental Research Institute, University of North Texas, Denton, TX, USA;

[6]Department of Microbiology and Immunology, Geisel School of Medicine at Dartmouth, Hanover, NH, USA

Abstract

Aquaporins are the predominant water-transporting proteins in vertebrates, but only a handful of studies have investigated aquaporin function in fish, particularly in mediating water permeability during salinity challenges. Even less is known about aquaporin function in hypoxia (low oxygen), which can profoundly affect gill function. Fish deprived of oxygen typically enlarge gill surface area and shrink the water-to-blood diffusion distance to facilitate oxygen uptake into the bloodstream. However, these alterations to gill morphology can result in unfavourable water and ion fluxes. Thus, there exists an osmorespiratory compromise, whereby fish must try to balance high branchial gas exchange with low ion and water permeability. Furthermore, the gills of seawater and freshwater teleosts have substantially different functions with respect to osmotic and ion fluxes; consequently, hypoxia can have very different effects according to the salinity of the environment. The purpose of this study was to determine what role aquaporins play in water permeability in the hypoxia-tolerant, euryhaline common killifish (*Fundulus heteroclitus*), in two important osmoregulatory organs – the gills and intestine. Using immunofluorescence, we localized aquaporin-3 protein to the basolateral and apical membranes of ionocytes and

[*]**AUTHOR AND ADDRESS FOR CORRESPONDENCE:** Dr. Chris M. Wood, Dept. of Zoology, University of British Columbia, Vancouver, B.C. V6T 1Z4, Canada, woodcm@zoology.ubc.ca, Tel: 1-604-827-1576, Fax: 1-604-822-2416.

[6].AUTHOR CONTRIBUTIONS

Conceptualization: CMW, IMR, KLS, and MG; Methodology: CMW, IMR, KLS, YW, and EMM; Validation: KLS, YW, and EMM; Formal analysis: IMR and CMW; Investigation: IMR, CMW.; Resources: CMW, MG, and BS; Data curation: IMR, CMW, KLS, YW, and EMM; Writing - original draft: IMR and CMW.; Writing - review & editing: IMR, CMW, KLS, YW, EMM, BS, and MG; Writing – approval of final version: IMR, CMW, and MG; Visualization: IMR; Supervision: CMW; Project administration: CMW, MG; Funding acquisition: CMW, MG, and BS.

enterocytes, respectively. Although hypoxia increased branchial aquaporin-3 mRNA expression in seawater and freshwater, protein abundance did not correlate. Indeed, hypoxia did not alter aquaporin-3 protein abundance in seawater and reduced it in the cell membranes of freshwater gills. Together, these observations suggest killifish aquaporin-3 contributes to reduced diffusive water flux during hypoxia and normoxic recovery in freshwater, and facilitates intestinal permeability in seawater and freshwater.

Graphical Abstract

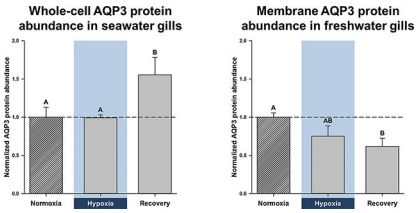

Keywords

Fundulus heteroclitus; gills; intestine; osmorespiratory compromise; western blot; immunofluorescence; mRNA; protein abundance; oxygen deprivation

1. INTRODUCTION

The gills of teleost fish are epithelial tissues in permanent contact with both the external and internal environments. Owing to these interactions, the composition of the external environment has a profound impact on the function of the gills. Indeed, seawater causes persistent water loss across the gills, because it is hyper-osmotic to extracellular fluids, whereas freshwater causes diffusive ion loss through the gills, because it is hypo-osmotic to extracellular fluids. Seawater teleosts compensate for this water loss by continuous uptake of salts and water by the intestine (i.e. solute-coupled water absorption), while the gills manage any excess plasma salt loads (Grosell, 2010; Larsen *et al.*, 2014). In contrast, freshwater teleost gills are the primary sites of salt and water uptake, while the kidneys eliminate excess water (Larsen *et al.*, 2014). Accordingly, the gills of freshwater teleosts are more permeable to water, whereas those of seawater fish stringently regulate salt fluxes (Isaia, 1984). Although seawater and freshwater teleosts maintain remarkably similar plasma osmolalities and ion levels, they do so using substantially different osmoregulatory strategies to preserve homeostasis (Larsen *et al.*, 2014).

Gill function can also be critically affected by shortages in dissolved oxygen (hypoxia), which can perturb osmoregulatory status. Most fish respond to hypoxia by morphological remodelling of the gills, which enlarges their surface area to shorten the diffusion distance of oxygen, but is commonly associated with a detrimental rise in ion and water permeability (Sardella and Brauner, 2007). Thus, there exists an “osmorespiratory compromise” that is defined as a trade-off between high permeability – to facilitate gas exchange across the gills – and low permeability – to constrain adverse ion and water fluxes (Nilsson, 1986; Sardella and Brauner, 2007).

Ion or water permeability is a dynamic component of branchial gas-exchange capacity that can be independently regulated over time, to maintain osmotic and ion homeostasis (Gonzalez and McDonald, 1992, 1994; Matey *et al.*, 2011; Swift and Lloyd, 1974; Wood *et al.*, 2009; Wood *et al.*, 2007). To some degree, however, many fish suffer from unfavourable ion and/or water fluxes, when there is a need to increase gas-exchange capacity, such as during intense exercise (Onukwufor and Wood, 2018; Postlethwaite and McDonald, 1995; Robertson *et al.*, 2015a; Robertson and Wood, 2014; Wood, 1988; Wood and Randall, 1973a, 1973b) or environmental hypoxia (Iftikar *et al.*, 2010; Matey *et al.*, 2008; Onukwufor and Wood, 2018; Robertson *et al.*, 2015b; Sollid *et al.*, 2003; Thomas *et al.*, 1986). Considering that fish allocate up to 10% of their energy budgets to osmoregulation (Bœuf and Payan, 2001) and that hypoxia can impair ATP-dependent transporters (which maintain ion gradients), changes in gill permeability can drastically disturb ion and water homeostasis.

Surprisingly, most studies on hypoxia-mediated changes in gill permeability have been conducted on freshwater fish, while only a handful exist on seawater fish (Farmer and Beamish, 1969; Hvas *et al.*, 2018; Stevens, 1972; Wood *et al.*, 2019). In the context of climate change, as the number of hypoxic dead zones in the oceans increase (Diaz and Rosenberg, 2008), it is vital that we learn more about the relationship between oxygen deprivation and gill permeability in marine fish. Furthermore, since water flux is one of the main variables when measuring gill permeability, it is also surprising that there are no reports on the roles that aquaporins might play in this process. Given that aquaporins are the main conduits for transcellular water transport in fish (Cerdà and Finn, 2010), obtaining this information would provide a more holistic understanding of branchial responses to variations in ambient salinity or dissolved oxygen.

Recently, we found that seawater killifish have tighter control over both branchial transcellular water permeability (unidirectional water-flux rates) and net water permeability (whole-body water-flux rates) than in freshwater, despite the much steeper osmotic gradient in seawater [Supplementary Table S1 (Wood *et al.*, 2019)]. These observations correlate with lower branchial aquaporin mRNA expression in several seawater-acclimated euryhaline fish that possibly serves to reduce diffusive water loss (Breves *et al.*, 2016; Cutler *et al.*, 2007; Lignot *et al.*, 2002; Madsen *et al.*, 2015; Tipsmark *et al.*, 2010). On the other hand, both hypoxia and normoxic recovery did not affect branchial water permeability in seawater, but considerably lowered it in freshwater [Table S1 (Wood *et al.*, 2019)]. This suggests that the killifish, which is known to be very hypoxia-tolerant, can reduce ion and water permeability, without sacrificing respiratory gas-exchange capacity – like some teleost species [e.g., the Amazonian oscar (Matey *et al.*, 2011; Robertson *et al.*, 2015a; Scott *et al.*, 2008; Wood *et al.*, 2009; Wood *et al.*, 2007)] – at least in freshwater (Giacomin *et al.*, 2019; Giacomin *et al.*, 2020). It is possible that hypoxia does not affect branchial water permeability in seawater killifish because it is already near its lower limit (Wood *et al.*, 2019). These data suggest that hypoxia might not affect branchial aquaporin protein abundance in seawater killifish, but suppress it in freshwater.

In the present study, we investigated the role aquaporin-3 (AQP3) might play in the branchial responses to hypoxia and normoxic recovery, both in seawater- and freshwater-

acclimated common killifish. Although a plethora of aquaporins have been identified in teleost fish (Cerdà and Finn, 2010; Madsen *et al.*, 2015; Tingaud-Sequeira *et al.*, 2010), we focused on AQP3 because many euryhaline species increase branchial AQP3 transcription when acclimated to freshwater from seawater (Cutler and Cramb, 2002; Deane and Woo, 2006; Lignot *et al.*, 2002; Madsen *et al.*, 2014; Moorman *et al.*, 2015; Tipsmark *et al.*, 2010; Tse *et al.*, 2006; Watanabe *et al.*, 2005), including common killifish (Jung *et al.*, 2012; Whitehead *et al.*, 2011a; Whitehead *et al.*, 2011b). Furthermore, a verified killifish AQP3 antibody is available (Jung *et al.*, 2012), which enabled us to quantify AQP3 protein abundance and immunofluorescence, along with measuring mRNA expression. Additionally, the teleost intestine also expresses AQP3 mRNA (Madsen *et al.*, 2014; Tipsmark *et al.*, 2010), but it distribution is not well characterized (Lignot *et al.*, 2002). Therefore, we used the killifish antibody to immunolocalize intestinal AQP3 in seawater and freshwater killifish.

We hypothesized that the reduction in diffusive water permeability in freshwater killifish during and following hypoxia observed in our previous study (Wood *et al.*, 2019) would be accompanied by a downregulation of AQP3 protein and mRNA levels in the branchial epithelium. We also hypothesized that as diffusive water permeability is generally higher in freshwater than seawater fish (Evans, 1967; Isaia, 1984; Potts and Fleming, 1970), the relative changes in AQP3 expression during hypoxia would be greater in the former and match our previous physiological data reported in Wood et al. (2019).

2. MATERIALS AND METHODS

2.1 Experimental animals

Experiments were performed over a three-year period (Feb-Apr 2015 to 2017). Adult common killifish of the northern subspecies (*Fundulus heteroclitus macrolepidotus*; 3–7 g, mixed sex) were collected the preceding October by beach-seining of local tidal flats (by Aquatic Research Organisms Ltd., Hampton, NH, USA) and held in their facility in 65% seawater, 22°C, for several months. After shipment to the University of Miami, they were held at 23–25°C, at a density of 30–50 animals per 50-l tanks, with flow-through dechlorinated freshwater or full-strength seawater, for at least one month prior to experiments. Fish were fed a daily ration of 1.5% body weight, with sinking pellets (50% protein; Purina Aquamax, Shoreview, MN, USA). The ionic composition of the food (Wood *et al.*, 2010) and of Miami freshwater and seawater (Wood and Grosell, 2008) have been reported earlier. Fish were fasted for 24 h prior to experiments, which were performed at the acclimation temperature. All procedures followed an approved University of Miami Animal Care Protocol (IACUC no. 13–225).

2.2 Experimental protocols

All experiments were performed with freshwater and seawater treatments in parallel, as described previously (Wood *et al.*, 2019). Briefly, all fish were subjected to identical pre-treatment and transfer protocols, to control for behavioural and physiological disturbances. Fish were placed into individual 250-ml Erlenmeyer flasks that were partially submerged in temperature-controlled wet tables (23–25°C), fitted with aeration tubing, and wrapped in black plastic shielding. The aeration tubing bubbled air or nitrogen into the flasks to achieve

normoxia (> 80% air saturation ≥ 16.5 kPa = 124 torr) or hypoxia (10% air saturation = 2.1 kPa = 15 torr; maintained within ±2% saturation during experiments), respectively. For water changes, pre-equilibrated normoxic or hypoxic water was flowed into each flask and target PO_2 was reached within 3 min. Fish were weighed after the completion of the experimental procedures.

In order to match the handling procedures in the ^3H_2O diffusive water flux experiments of Wood et al. (2019), fish were first subjected to a 6–8-h sham-loading period, before they were transferred to the individual flasks, for sampling after 1 h of normoxia, 3 h of hypoxia, or 3 h of normoxic recovery. 3 h of hypoxia was selected, as we have shown it alters branchial water permeability in killifish (Wood *et al.*, 2019). At these times, the fish were quickly euthanized by overdose with neutralized MS-222 (0.8 g l^{-1}; pre-equilibrated to the appropriate PO_2) and the eight gill arches were quickly dissected out. For western blotting (N = 10 in both normoxia and hypoxia, N = 8 in normoxic recovery), the gill arches were rinsed and blotted, and then placed in sealed cryovials, flash-frozen in liquid N_2, and stored at −80°C for later analysis. To ensure sufficient protein for western blotting, the gill arches from two fish were subsequently pooled, so effective N-values were 5 in normoxia and hypoxia, and 4 in normoxic recovery. For mRNA expression and immunohistochemistry, the gill arches from separate groups of fish (N = 6 per treatment) were rinsed in Cortland saline and blotted; the left arches were put into RNA*later*™ (Ambion, Austin, TX, U.S.A.) and stored at 4°C for later real-time, quantitative polymerase chain reaction (qPCR) analysis, and the right ones into Z-fix™ (buffered zinc formalin fixative; Anatech Ltd., Battle Creek, MI, USA) and stored at room temperature for later immunohistochemistry. The intestine was similarly rinsed, blotted, and cut into several small sections, some of which were preserved in RNA*later*™ and some in Z-fix™.

2.3 Western blotting

Membrane isolations used a modified procedure described previously (Tresguerres *et al.*, 2005). Briefly, frozen gill samples were ground to a fine powder, with a liquid N_2-chilled CryoGrinder (OPS Diagnostics, Lebanon, NJ, USA). Approximately 1 ml of homogenization buffer [250 mM sucrose, 1 mM EDTA, 30 mM tris, 1x HALT protease inhibitor cocktail (Thermo Fisher Scientific, Rockford, IL, USA), pH 7.4] was added for every 400 μg of ground tissue, and cells were lysed via sonication on ice, with two 10-s pulses, allowing 30 s to cool between pulses. The cell lysates were cleared via a 10-min, 3000-g spin at 4°C, after which the supernatant was retained, and a small aliquot was taken as the whole-cell lysate. Membranes were pelleted from the remaining lysate via a 60-min, 20,800-g spin at 4°C. The resulting supernatant was retained as the cytoplasmic fraction, and the pellet was resuspended in 1x RIPA buffer (150 mM NaCl, 50 mM tris, 1% Triton X-100, 0.5% sodium deoxycholate, 0.1% sodium dodecyl sulfate, pH 7.6). Protein concentrations were determined by Pierce BCA assay (Thermo Fisher Scientific) and stored at −80 °C until further analysis.

Isolated protein samples (20 μg) were separated on 4–15% tris-glycine gels (Bio-Rad Laboratories, Hercules, CA, USA) and transferred to polyvinylidene fluoride (PVDF) membranes. Membranes were blocked in Pierce Protein-Free Blocking Buffer (Thermo

Fisher Scientific), for 1 h, at room temperature, followed by overnight incubation, at 5°C, in dilute (1:1000) killifish AQP3 antibody (Jung *et al.*, 2012) or a commercially available, rabbit polyclonal Na^+/K^+-ATPase (NKA) antibody (1:1000; cat. no. SC-28800, Santa Cruz Biotechnology, Dallas, TX, USA). Blots were then probed with horseradish peroxidase conjugated donkey anti-rabbit secondary antibody (1:25,000; cat. no. SC-2313, Santa Cruz Biotechnology), for 1 h, at room temperature. Blots were developed in SuperSignal West Femto Maximum Sensitivity Substrate (Thermo Fisher Scientific) and imaged on a C-DiGit scanner (LI-COR Biosciences, Lincoln, NE, USA). AQP3 band intensity was determined via Image Studio Lite (version 5.0.21; LI-COR Biosciences) and normalized to total protein via subsequent Coomassie Brilliant Blue staining of the blot (also determined using Image Studio Lite).

2.4 cDNA synthesis and real-time, quantitative PCR (qPCR)

Total RNA was extracted from tissue samples using RNA STAT-60 solution (Tel-Test, Friendsworth, TX, USA) and treated with DNase I (Turbo DNA-free Kit; Thermo Fisher Scientific). RNA concentration and quality were measured with a Spectra-Drop (SpectraMax Plus 384, Molecular Devices) and confirmed for integrity by gel electrophoresis. cDNA was then synthesized using SuperScript IV First-Strand Synthesis System (Invitrogen, Waltham, MA, USA) and final products were diluted tenfold in sterile water. A mixture of equivalent volumes from random cDNA samples was prepared as a calibrator.

The qPCR primers (Table S2) were designed using sequence information from NCBI. Products were amplified using a Taq PCR Core Kit (Qiagen, Germantown, MD, USA), cloned using a TOPO-TA Cloning Kit (Thermo Fisher Scientific), and sequenced to validate target specificity. All qPCR experiments were performed in triplicate (6–7 biological replicates) in the Stratagene Mx4000 instrument (Stragene, San Diego, CA, USA), using Power SYBR Green Master Mix (Thermo Fisher Scientific). Cycling was as follows: 95°C (10 min), 40 cycles at 95°C (30 s), 58°C (30 s), and 72°C (30 s). Specificity of target amplicons was verified by melting-curve analysis and gel electrophoresis. Relative mRNA expression levels were calculated using the PCR Miner software (Zhao and Fernald, 2005), normalized to EF1α mRNA expression (which was unaltered by experimental treatments), and expressed relative to the treatment/tissue exhibiting the lowest level of expression. Further details are summarized in the Electronic Supplementary Material.

2.5 Immunohistochemistry

Following fixation in Z-fix™, gill tissues were immersed in 70% ethanol (~1:20 w/v), dehydrated in ascending grades of ethanol, washed in butanol and Histochoice™ clearing reagent (Amresco, Solon, OH, USA), and finally immersed four times in Paraplast Plus™ tissue-embedding medium (Leica Biosystems, Richmond, IL, USA), after which tissues were embedded in tissue molds with Paraplast. Tissues were sectioned at 4 μm, using a Leitz model 1512 microtome (Grand Rapids, MI, USA) and mounted onto poly-L-lysine-coated slides. For steps on how slides were prepared for antibody treatment (i.e., Paraplast removal, rehydration, revealing antigenic sites, and non-specific antigenic blocking), see the Electronic Supplementary Material.

The primary antibodies were monoclonal mouse CFTR (cat. no. MAB25031, R&D Systems, Minneapolis, MN, USA) and polyclonal rabbit NKA (cat. no. SC-28800, Santa Cruz Biotechnology). The CFTR antibody has been validated in the Gulf toadfish intestine (Ruhr *et al.*, 2014; Ruhr *et al.*, 2018) and killifish gills (Marshall *et al.*, 2002) by western blotting and immunohistochemistry. Likewise, the NKA antibody has been validated in the Gulf toadfish intestine (Ruhr *et al.*, 2014; Ruhr *et al.*, 2018). The killifish aquaporin-3 antibody (kfAQP3; IACUC registration 50-R-0013) was designed and validated in killifish by western blotting (Jung *et al.*, 2012). To double-stain tissues, the antibodies were diluted to 10 μg ml $^{-1}$, in modified blocking PBS (PBS with 0.5% skim milk, 1% BSA, and 0.05% Tween-20). Slides were incubated overnight with primary antibodies, in a humidified slide-box, with gentle agitation, on an oscillating table (5°C). The next morning, they were rinsed twice in PBS containing 0.05% Tween-20 and once in normal PBS.

Application of secondary antibodies was done in the dark. The secondary antibodies were donkey anti-mouse IgG secondary antibody for CFTR (Alexa Fluor 488; cat. no. AB_2556542, Thermo Fisher Scientific) and donkey anti-rabbit IgG secondary antibody for NKA or AQP3 (Alexa Fluor 568; cat. no. A10042, Thermo Fisher Scientific), diluted to 10 μg ml^{-1} (in blocking PBS). Slides were incubated in a humidified slide box for 1 h, at 37°C, after which they were rinsed as before. ProLong™ Gold Antifade Reagent (Thermo Fisher Scientific) was used to adhere the coverslips to each slide. Control slides were treated equally, apart from primary antibody.

Slides were observed with a fluorescent microscope (Olympus, Center Valley, PA, USA), and images were taken with an attached camera (Retiga EXi, Fast 1394, QImaging, Surrey, B.C., Canada) and Olympus u-tvo.5xc-2 camera mount, using the same settings. Fiji (Schindelin *et al.*, 2012), iVision, and Gimp software were used to analyze the images quantitatively as relative corrected fluorescence in arbitrary units (a.u.). Further details are summarized in the Electronic Supplementary Material.

2.6 Statistical analyses

Data were initially checked for normality with a Shapiro-Wilk test and for homogeneity with a Bartlett's chi-square test; when necessary, data were converted using logarithmic or square-root transformations. Data were analyzed for statistical significances by generalized linear models, using Bonferroni corrections for pairwise comparisons, with SPSS 25 (IBM, Armonk, NY, USA). All tests were two-tailed and significance was accepted when $P \leq 0.05$. All data are reported as means ± SEM. Statistical support for the findings (i.e. test statistics, degrees of freedom, and SPSS-adjusted P-values) are given in the Electronic Supplementary Material (Tables S3 to S6).

3 RESULTS

3.1 Abundance of branchial transport proteins in seawater

Enrichment of NKA protein in the gill [which is known to reside primarily in the basolateral membrane of killifish (Karnaky Jr *et al.*, 1976)] was approximately 5-fold higher in the cell-membrane fraction, relative to whole-cell lysates (normalized values of 5.39 ± 0.86 vs. 1 ±

0.18), suggesting the membrane enrichment was successful. For internal consistency, the whole-cell, cytoplasm, and membrane fractions of gills from normoxic, hypoxic, and recovery treatments within the same salinity (freshwater or seawater) were each run on the same gel (separate gels for each fraction), and data were normalized to the normoxic treatment for that fraction, as shown in Fig. 1 (original blots are shown in Supplementary Fig. S1). Gills from different salinities were also run on different gels, thus, the data can only be quantitatively compared among treatments within each fraction, and not between salinities or between fractions. However, there was enough of the whole-cell fraction from the two salinities to also run both on the same gel, which revealed no significant difference in AQP3 protein abundance between salinities (normalized values of 1 ± 0.08 in freshwater vs. 1.93 ± 0.62 in seawater; $P = 0.13$).

Branchial whole-cell AQP3 protein abundance in seawater was significantly higher after recovery than during either normoxia or hypoxia, but no significant differences were found in the cytoplasmic or membrane fractions (Fig. 1A, B, and C). Elevated whole-cell AQP3 protein abundance in recovered fish gills might be due to higher levels of mRNA in hypoxia (Fig. 2A). Indeed, by the end of 3 h hypoxia, branchial AQP3 mRNA expression in seawater had increased to 290% of normoxic levels.

Furthermore, we also quantified AQP3 protein immunofluorescence in the lamellae and interlamellae of the seawater gills, since this type of spatial resolution was not possible with western blotting. This technique demonstrated that hypoxia did not affect total AQP3 immunofluorescence (i.e., combined signal intensity in the lamellae and interlamellae; Fig. 3A and B). However, the interlamellar regions of normoxic gills had significantly higher AQP3 immunofluorescence than the lamellar regions. This is exemplified by the very different scales of the y-axes (Fig. 3A and B).

In addition to using immunohistochemistry to confirm the presence of AQP3 in seawater killifish gills, we also used CFTR and NKA immunofluorescent antibodies to indicate the membrane-specific location of AQP3. CFTR was abundant in the apical and sub-apical regions of normoxic gills, but less abundant in hypoxic gills (Fig. 4B, C, E, and F). In general, CFTR was expressed in cells where NKA expression was also prominent, likely ionocytes (a.k.a. chloride cells/mitochondria-rich cells; an example of an apical crypt, composed of high CFTR abundance, on an ionocyte is shown in the inset of Fig. 4C), but only some of the NKA-rich cells expressed CFTR. In both normoxic and hypoxic gills, NKA was localized to the basolateral membrane of the interlamellae and, in hypoxic gills, it was also distributed in the outer margins of the lamellae (Fig. 4C and F).

AQP3 immunofluorescence had a similar pattern of expression as NKA, in seawater killifish. AQP3 was found on the outer borders of the lamellae and more markedly in the interlamellar regions, where it was clearly localized to the basolateral membranes (Fig. 4A, B, D, and E). On the margins of the lamellae, the situation was less clear; while the pattern was similar to that of NKA, it is possible that AQP3 is expressed both apically and basolaterally. Considering that brightfield images showed red-blood cells spanning almost the entire width of the lamellae, we could not determine the position of either membrane. Moreover, it is also possible that branchial AQP3 is predominantly sub-basolateral or

vesicle-bound, which provides an explanation for why AQP3 protein abundance is higher in the whole-cell fraction of recovery fish, but not in the corresponding membrane fraction.

3.2 Abundance of branchial transport proteins in freshwater

In freshwater gills, there was a trend for reduced AQP3 protein abundance during hypoxia and particularly recovery in all three fractions (Fig. 1D, E, and F). In the membrane fraction, the reduction in AQP3 protein abundance was close to significance in hypoxia ($P = 0.065$) and significantly lower in recovery (Fig. 1F). As with the seawater gills, lower AQP3 protein abundance in hypoxia and recovery was also accompanied by a paradoxical, hypoxia-mediated elevation in AQP3 mRNA; indeed, it amounted to a significant, 67% increase in mRNA expression, relative to control normoxic gills (Fig. 2B). Additionally, hypoxia caused significant reductions in total branchial AQP3 immunofluorescence, a decrease that was also significant in the lamellar regions (Fig. 3C and D). Furthermore, the interlamellae of both normoxic and hypoxic gills displayed significantly more AQP3 immunofluorescence than their lamellar counterparts (Fig. 3C and D).

Freshwater gills showed little CFTR immunofluorescence (Fig. 4H and K), whereas NKA was abundant in the basolateral membrane of the interlamellae and distributed in the outer margins of the lamellae, which seemed unaffected by hypoxia (Fig. 4I and L). AQP3 was also found on the outer borders of the lamellae and plentifully in the interlamellae in both normoxia and hypoxia (Fig. 4G, H, J, and K). Like in seawater, freshwater gills displayed AQP3 immunofluorescence in the basolateral membrane, but we could not determine its cellular location in the lamellae (Fig. 4G, H, J, and K).

3.3 Effect of salinity on branchial AQP3 protein abundance

Although we did not find differences in branchial AQP3 protein abundance between salinity acclimations, aside from those of normoxic whole-cell fractions (see above), we observed qualitative differences between seawater and freshwater. The gills of seawater-acclimated fish did not alter AQP3 protein levels in hypoxia and responded to normoxic recovery by a general trend for increased AQP3 protein abundance (Fig. 1A and C), whereas freshwater-acclimated fish subjected to hypoxia and recovery tended to depress AQP3 protein abundance (Fig. 1D, E, and F). Quantitatively, freshwater acclimation resulted in significantly higher total AQP3 mRNA expression and total immunofluorescence (both P-values ≥ 0.001), with both normoxic and hypoxic freshwater fish gills exhibiting significantly more AQP3 mRNA (Fig. 2A and B). Furthermore, freshwater fish lamellae in normoxia and interlamellae in hypoxia displayed significantly greater AQP3 immunofluorescence than their seawater counterparts (Fig. 3).

3.4 Distribution of intestinal transport proteins

Intestinal AQP3 mRNA expression was substantially lower than in the gills and hypoxia did not alter gene expression in either salinity (Fig. 5C and D). Nevertheless, the intestine of seawater and freshwater fish displayed AQP3 protein immunofluorescence and we used the immunofluorescent antibodies to localize AQP3 and NKA; material from the hypoxic exposures was not processed. Although we did not quantify the specific intensity of AQP3 immunofluorescence, there appeared to be no differences between the two salinity

acclimation groups. AQP3 was abundant in the apical membrane of the enterocytes and in the mucous cells (Fig. 5 A, B, E, and F).

4. DISCUSSION

Numerous studies on fish show that oxygen limitation – either due to environmental hypoxia or strenuous exercise – alters the permeability of the gills. Fish enlarge gill surface area to improve gas exchange across the epithelium, but it is often accompanied by unfavourable ion and water fluxes (see Introduction). This osmorespiratory compromise has been investigated extensively in freshwater, but very few studies have attempted to characterize this response in seawater fish (Farmer and Beamish, 1969; Hvas *et al.*, 2018; Stevens, 1972; Wood *et al.*, 2019) and none have investigated the possible roles aquaporins play.

Here we show, for the first time, that branchial aquaporin-3 (AQP3) protein abundance and mRNA expression change in a salinity-dependent manner, when common killifish are subjected to hypoxia and normoxic recovery. Our results suggest that there is general agreement with AQP3 protein abundance during hypoxia in seawater and freshwater (Fig. 1A and F, Fig. 3) and gill diffusive water fluxes, which is a proxy for transcellular water permeability (Table S1, Wood *et al.*, 2019). Furthermore, our data also suggest that water transport must be strictly regulated during recovery, given that seawater killifish gills increase AQP3 protein abundance, but do not alter transcellular water permeability, while freshwater killifish gills lower both AQP3 protein abundance and transcellular water permeability even further, rather than returning to normoxic levels (Fig. 1A and F, Fig. 3, Table S1). Importantly, our results suggest that water-permeability changes in freshwater are associated with modifications in AQP3 protein abundance during and after acute hypoxia.

4.1 Modulation of AQP3 in normoxic seawater and freshwater

Fluctuations in salinity often alter the distribution and production of branchial ion transporters (Larsen *et al.*, 2014). In killifish gills, for example, freshwater elevates apical Na^+/Cl^--cotransporter (NCC2) protein and mRNA levels – likely to facilitate ion absorption – and inhibits apical CFTR and basolateral $Na^+/K^+/2Cl^-$-cotransporter (NKCC1) mRNA expression – likely to suppress ion secretion (Breves *et al.*, 2020). Furthermore, freshwater also increases branchial AQP3 protein abundance and/or gene expression in euryhaline fish (Cutler and Cramb, 2002; Deane and Woo, 2006; Lignot *et al.*, 2002; Madsen *et al.*, 2014; Moorman *et al.*, 2015; Tipsmark *et al.*, 2010; Tse *et al.*, 2006; Watanabe *et al.*, 2005). In combination, such alterations are linked with modified water transport across the gills (Larsen *et al.*, 2014). Likewise, we found higher AQP3 protein immunofluorescence and mRNA expression in the gills of killifish acclimated to freshwater than to seawater (Fig. 2 and Fig. 3); the greater mRNA levels in freshwater killifish agree with earlier reports on common killifish (Jung *et al.*, 2012; Whitehead *et al.*, 2011a; Whitehead *et al.*, 2011b). Our observations also parallel the faster control rates of diffusive water exchange (i.e. transcellular water fluxes) in freshwater killifish (Table S1; Wood *et al.*, 2019). However, despite 6-fold differences in mRNA expression, there were no differences in seawater versus freshwater whole-cell AQP3 protein abundance, which agree with earlier reports on the killifish (Jung *et al.*, 2012) and the Mozambique tilapia (Watanabe *et al.*, 2005). Conversely,

most other teleost studies have found freshwater acclimation raises branchial AQP3 protein levels, although these reports show that relative changes in protein abundance are generally smaller than differences in mRNA expression (Deane and Woo, 2006; Lignot *et al.*, 2002; Tse *et al.*, 2006; Watanabe *et al.*, 2005). Such mismatches between mRNA expression and protein abundance are very common (Jung *et al.*, 2012). A variety of factors act to buffer protein concentrations from variations in mRNA levels (Liu *et al.*, 2016); furthermore, post-translational modification, which can alter aquaporin function, is well-documented (Moeller *et al.*, 2011), and would not be reflected in the western-blot data.

In addition to quantifying changes in protein abundance by western blotting, we also used the kfAQP3 antibody to measure AQP3 protein immunofluorescence in killifish gills. This technique revealed that freshwater acclimation enhanced AQP3 protein immunofluorescence in the gills, particularly under normoxic conditions in the interlamellae (Fig.3). Thus, these results suggest that membrane abundance of AQP3 protein is greater in freshwater, even though gill cells contain roughly equal amounts of AQP3 protein. Such disparities in protein distribution between treatments are not unusual; indeed, branchial CFTR protein abundance is the same in seawater and freshwater killifish, yet more CFTR is found on the cell membranes of seawater gills (Shaw *et al.*, 2008). Taken together, the larger amounts of AQP3 immunofluorescence and mRNA expression in freshwater correlate with the higher diffusive water fluxes in freshwater (Table S1) and suggest a central role for AQP3 in regulating water permeability in killifish gills.

With respect to its branchial distribution in seawater and freshwater, we found AQP3 localized to the basolateral membranes in the interlamellar regions – where ionocytes are most plentiful – and largely to these same membranes in the lamellae – where pavement cells are predominant – though, it is possible that there was also an apical component in the latter (Fig. 4). This basolateral distribution in the ionocytes, as well as occurrence in pavement cells, agrees with previous reports (Breves *et al.*, 2016; Brunelli *et al.*, 2010; Cutler *et al.*, 2007; Lignot *et al.*, 2002; Madsen *et al.*, 2015; Watanabe *et al.*, 2005). However, the cellular distribution of AQP3 in the gills differed in one important aspect from that previously reported in killifish (Jung *et al.*, 2012). Using the identical kfAQP3 antibody in the same species, we detected AQP3 protein immunofluorescence at the outer borders of the lamellae only (undoubtedly in the pavement cells), whereas the previous study reported AQP3 protein immunofluorescence only in internal pillar cells of the lamellae (Jung *et al.*, 2012). We are aware of no other reports of aquaporins in pillar cells, and the reason for this discrepancy is unknown. Nevertheless, our results agree with the prior report on killifish (Jung *et al.*, 2012) showing the greatest signal in the interlamellar regions (Fig. 3B and D), where ionocytes are most abundant, with co-localization of AQP3 and NKA in these cells (Fig. 4). There is also agreement that AQP3 expression in the lamellae was greater with freshwater acclimation, at least under normoxia (Fig. 3A and C). However, in contrast to the previous killifish study (Jung *et al.*, 2012), we saw an increased signal in ionocytes in the interlamellar region with freshwater acclimation (Fig. 3B and D). Again, the prevalence of AQP3 in the lamellae – where surface area is high – in freshwater fits with the greater rate of diffusive water exchange than in seawater under normoxia (Table S1; Wood *et al.*, 2019).

4.2 Hypoxia alters branchial AQP3 protein abundance in freshwater, but not seawater

In the gills of freshwater killifish, hypoxia lowered AQP3 protein abundance (Fig. 1) and immunofluorescence, especially in the lamellae (Fig. 3), in support of our hypothesis. These changes in protein abundance mirror the substantial reduction in transcellular water permeability in freshwater (Table S1; Wood *et al.*, 2019), which suggests AQP3 is involved in branchial water transport. On the other hand, hypoxia had no effect on AQP3 protein abundance and immunofluorescence in seawater (Fig. 1 and Fig. 2), which might explain why transcellular water permeability also does not change (Table S1). In both seawater and freshwater, hypoxia led to greater AQP3 mRNA expression (Fig. 2) that was not reflected by corresponding increases in protein abundance or immunofluorescence, perhaps as a result of post-transcriptional modifications (Liu *et al.*, 2016).

Although AQP3 protein abundance and transcellular water permeability are unaffected in hypoxic seawater, paracellular permeability of the gills is considerably reduced, in both seawater and freshwater (Table S1). As stated previously, transcellular water permeability remains unchanged during hypoxia in seawater killifish, possibly because this rate is already at its lower limit in seawater gills. Consequently, by impeding the permeability of the paracellular route, even less water will be lost to the environment. In freshwater, limiting both the transcellular and paracellular permeabilities of the gills (Table S1) will reduce unfavourable water entry. The transcellular permeability reduction would be facilitated by lower AQP3 protein abundance in the cell membrane (Fig. 1F). Furthermore, seeing as AQP3 is an aquaglyceroporin that is also permeable to other molecules – glycerol, hydrogen peroxide, urea, and ammonia (Litman *et al.*, 2009; Miller *et al.*, 2010; Verkman, 2012) – reducing AQP3 membrane abundance and, thus, solute efflux might be advantageous. For example, attenuating glycerol loss could be energetically useful, given the switch to triglyceride metabolism during hypoxia (Gracey *et al.*, 2011). As a result, osmoregulatory costs are minimized by both seawater and freshwater killifish in hypoxic water, given that oxygen permeability is likely greatly increased in hypoxia (Giacomin *et al.*, 2019).

We are aware of no other reports on fish investigating the effect hypoxia might have on branchial protein or mRNA levels of aquaporins. Within the 3-h timeframe of our study, hypoxia would not be expected to cause large changes in absolute AQP3 protein concentration (Liu *et al.*, 2016), and, indeed, this is what we saw (Fig. 1). Conversely, owing to the medical implications of perturbed aquaporin function in humans (Soveral *et al.*, 2018), pre-clinical studies show that oxygen deprivation can suppress aquaporin protein synthesis [e.g., in rodent brain cells (Baronio *et al.*, 2013; Yamamoto *et al.*, 2001)], including AQP3 in the human placenta (Szpilbarg and Damiano, 2017). These reductions might be adaptative responses that limit cellular water flux or programmed cell death. Thus, there seems to be general agreement that vertebrates subjected to oxygen deprivation alter aquaporin protein abundance to reduce osmoregulatory stress.

4.3 Normoxic recovery alters branchial AQP3 protein abundance differently in seawater and freshwater

Killifish subjected to normoxic recovery exhibited changes in branchial AQP3 protein abundance that were in opposite directions in seawater and freshwater. In seawater,

normoxic recovery increased whole-cell AQP3 protein abundance in the gills, but these higher levels of AQP3 were not reflected in the cell membrane (Fig. 1). This suggests that AQP3 insertion into the cell membrane does not match its cellular production and/or that gill cells are recycling membrane-bound AQP3 with newly synthesized proteins. Accordingly, the unchanged levels of AQP3 protein in the cell membrane could account for the unaffected transcellular water fluxes observed in seawater gills (Table S1). Paradoxically, normoxic recovery further lowered AQP3 protein abundance in the cell membrane of freshwater gills (Fig. 1), which accompanies a continued reduction in transcellular water permeability (Table S1). We might expect both branchial AQP3 membrane protein abundance and transcellular water permeability be restored to their pre-hypoxic levels in recovery, but this was not the case. This result suggests that freshwater killifish actively restrict branchial permeability when returned to normoxia, at least during the time-course of our study. Moreover, the elevation in AQP3 mRNA expression in both hypoxic seawater and freshwater gills could serve as a preparatory event for enhanced protein production that is beyond the time-course of our study (Liu *et al.*, 2016), although this merits further study. In addition, future studies should explore branchial AQP3 mRNA expression and protein immunofluorescence, morphology, and ion fluxes during hypoxia and in normoxic recovery, to further inform us of the role(s) that aquaporins and other channel proteins play in the physiology of killifish gills.

4.4 Seawater and freshwater intestines express AQP3 equally

The intestine of seawater teleosts is the organ responsible for water uptake and plays a minor, yet important, role in water influx in freshwater (Grosell, 2010; Marshall and Grosell, 2006). Moreover, the major pathway for fluid absorption in the killifish intestine is transcellular in both seawater and freshwater (Wood and Grosell, 2012). Therefore, we also investigated the distribution of AQP3 in the intestine of killifish acclimated to seawater or freshwater. In contrast to the gills, AQP3 in the intestine was localized to the apical membranes of the enterocytes and to mucous cells (Fig. 5). This pattern only partly agrees with observations of the eel gut (Lignot *et al.*, 2002), in which AQP3 expression was reported in only some mucous (“goblet” cells) and macrophages, and not in the enterocytes. Moreover, AQP3 has been found in the gut of other teleost species, but its physiological role has not been extensively studied [for review (Madsen *et al.*, 2015)]. Regardless, all cells require water and must have the capacity to transport it. Thus, the presence of AQP3 in the killifish intestine is not surprising, but its physiological role should be studied further.

4.5 Perspective: the potential role of AQP3 in the osmorespiratory compromise during hypoxia

Overall, our data support the conclusion that *F. heteroclitus* is a hypoxia-tolerant species (see Introduction) that can reduce branchial ion and water permeability, while preserving respiratory gas-exchange capacity (Giacomin *et al.*, 2019; Giacomin *et al.*, 2020; Wood *et al.*, 2019). With respect to regulating water transport, our data suggest that AQP3 plays a role during acute hypoxia and normoxic recovery, at least in freshwater-acclimated killifish. Under normoxic conditions, branchial AQP3 is likely involved in regulating water entry/exit, cell volume, or osmosensing (Cutler *et al.*, 2007; Madsen *et al.*, 2015; Watanabe *et al.*, 2005). We also show that AQP3 is present in the apical membrane of enterocytes in seawater

and freshwater, indicating an involvement in intestinal permeability. Although AQP1a1 has been implicated in diffusive water exchange in larval zebrafish (Kwong *et al.*, 2013) and many other aquaporins occur in fish, we have provided evidence that changes in branchial AQP3 protein abundance correlate with fluctuations in diffusive water fluxes in freshwater killifish. Considering the importance of branchial water permeability, it is surprising how little is known about the regulation and physiological function of aquaporins in the over-30,000 species of teleost fish worldwide.

Supplementary Material

Refer to Web version on PubMed Central for supplementary material.

ACKNOWLEDGEMENTS

We thank Dr. Mike Schmale (University of Miami) for use of his imaging facility and advice on microscopy, Dr. Dawoon Jung (Korea Environment Institute) for advice on immunohistochemistry, and Dr. Patricia Schulte (University of British Columbia) for advice on gene expression.

7. FUNDING

Supported by Natural Sciences and Engineering Research Council of Canada (NSERC) Discovery Grants to CMW (RGPIN-2017-03843, RGPIN/473-2012), and by NIEHS grant P42 ES007373 to BS. KLS was partly supported by a University of Miami Maytag Fellowship. MG is a Maytag Professor of Ichthyology.

8. REFERENCES

Baronio D, Martinez D, Fiori CZ, Bambini-Junior V, Forgiarini LF, Pase da Rosa D, Kim LJ, and Cerski MR (2013). Altered aquaporins in the brains of mice submitted to intermittent hypoxia model of sleep apnea. Respir Physiol Neurobiol, 185(2), 217–221. doi:10.1016/j.resp.2012.10.012 [PubMed: 23123204]

Bœuf G and Payan P (2001). How should salinity influence fish growth? Comp Biochem Physiol C Toxicol Pharmacol, 130(4), 411–423. doi:10.1016/s1532-0456(01)00268-x [PubMed: 11738629]

Breves JP, Inokuchi M, Yamaguchi Y, Seale AP, Hunt BL, Watanabe S, Lerner DT, Kaneko T, and Grau EG (2016). Hormonal regulation of aquaporin 3: opposing actions of prolactin and cortisol in tilapia gill. J Endocrinol, 230(3), 325–337. doi:10.1530/JOE-16-0162 [PubMed: 27402066]

Breves JP, Starling JA, Popovski CM, Doud JM, and Tipsmark CK (2020). Salinity-dependent expression of ncc2 in opercular epithelium and gill of mummichog (*Fundulus heteroclitus*). J Comp Physiol B, 190(2), 219–230. doi:10.1007/s00360-020-01260-x [PubMed: 31980891]

Brunelli E, Mauceri A, Salvatore F, Giannetto A, Maisano M, and Tripepi S (2010). Localization of aquaporin 1 and 3 in the gills of the rainbow wrasse, *Coris julis*. Acta Histochem, 112(3), 251–258. doi:10.1016/j.acthis.2008.11.030 [PubMed: 19428055]

Cerdà J and Finn RN (2010). Piscine aquaporins: an overview of recent advances. J Exp Zool A Ecol Genet Physiol, 313(10), 623–650. doi:10.1002/jez.634 [PubMed: 20717996]

Cutler CP and Cramb G (2002). Branchial expression of an aquaporin 3 (AQP-3) homologue is downregulated in the European eel *Anguilla anguilla* following seawater acclimation. J Exp Biol, 205(Pt 17), 2643–2651. [PubMed: 12151370]

Cutler CP, Martinez AS, and Cramb G (2007). The role of aquaporin 3 in teleost fish. Comp Biochem Physiol A Mol Integr Physiol, 148(1), 82–91. doi:10.1016/j.cbpa.2006.09.022 [PubMed: 17126580]

Deane EE and Woo NY (2006). Tissue distribution, effects of salinity acclimation, and ontogeny of aquaporin 3 in the marine teleost, silver sea bream (*Sparus sarba*). Mar Biotechnol, 8(6), 663–671. doi:10.1007/s10126-006-6001-0 [PubMed: 16909214]

Diaz RJ and Rosenberg R (2008). Spreading dead zones and consequences for marine ecosystems. Science, 321(5891), 926–929. doi:10.1126/science.1156401 [PubMed: 18703733]

Evans DH (1967). Sodium, chloride, and water balance of the intertidal teleost, *Xiphister atropurpureus*: III. The roles of simple diffusion, exchange diffusion, osmosis, and active transport. J Exp Biol, 47(Pt 3), 525–534. [PubMed: 5592420]

Farmer GJ and Beamish FWH (1969). Oxygen consumption of Tilapia nilotica in relation to swimming speed and salinity. J Fish Res Board Can, 26(11), 2807–2821. doi:10.1139/f69-277

Giacomin M, Bryant HJ, Val AL, Schulte PM, and Wood CM (2019). The osmorespiratory compromise: physiological responses and tolerance to hypoxia are affected by salinity acclimation in the euryhaline Atlantic killifish (*Fundulus heteroclitus*). J Exp Biol, 222(Pt 19), jeb206599. doi:10.1242/jeb.206599

Giacomin M, Onukwufor JO, Schulte PM, and Wood CM (2020). Ionoregulatory aspects of the hypoxia-induced osmorespiratory compromise in the euryhaline Atlantic killifish (*Fundulus heteroclitus*): the effects of salinity. J Exp Biol, Accepted.

Gonzalez RJ and McDonald DG (1992). The relationship between oxygen consumption and ion loss in a freshwater fish. J Exp Biol, 163(Pt 1), 317–332.

Gonzalez RJ and Mcdonald DG (1994). The relationship between oxygen uptake and ion loss in fish from diverse habitats. J Exp Biol, 190(Pt 1), 95–108. [PubMed: 9317409]

Gracey AY, Lee TH, Higashi RM, and Fan T (2011). Hypoxia-induced mobilization of stored triglycerides in the euryoxic goby *Gillichthys mirabilis*. J Exp Biol, 214(Pt 18), 3005–3012. doi:10.1242/jeb.059907 [PubMed: 21865512]

Grosell M (2010). The role of the gastrointestinal tract in salt and water balance In Grosell M, Farrell AP, and Brauner CJ (Eds.), Fish Physiology (Vol. 30: The Multifunctional Gut of Fish, pp. 135–164). Oxford, U.K.: Academic Press.

Hvas M, Nilsen TO, and Oppedal F (2018). Oxygen uptake and osmotic balance of Atlantic salmon in relation to exercise and salinity acclimation. Front Mar Sci, 5, 368. doi:10.3389/fmars.2018.00368

Iftikar FI, Matey V, and Wood CM (2010). The ionoregulatory responses to hypoxia in the freshwater rainbow trout, *Oncorhynchus mykiss*. Physiol Biochem Zool, 83(2), 343–355. doi:10.1086/648566 [PubMed: 20095822]

Isaia J (1984). Water and Nonelectrolyte Permeation In Hoar WS and Randall DJ (Eds.), Fish physiology (Vol. 10, Part B, pp. 1–38): Elsevier.

Jung D, Sato JD, Shaw JR, and Stanton BA (2012). Expression of aquaporin 3 in gills of the Atlantic killifish (*Fundulus heteroclitus*): Effects of seawater acclimation. Comp Biochem Physiol A Mol Integr Physiol, 161(3), 320–326. doi:10.1016/j.cbpa.2011.11.014 [PubMed: 22193757]

Karnaky KK Jr, Kinter LB, Kinter WB, and Stirling CE (1976). Teleost chloride cell. II. Autoradiographic localization of gill Na, K-ATPase in killifish *Fundulus heteroclitus* adapted to low and high salinity environments. J Cell Biol, 70(1), 157–177. doi:10.1083/jcb.70.1.157 [PubMed: 132451]

Kwong RW, Kumai Y, and Perry SF (2013). The role of aquaporin and tight junction proteins in the regulation of water movement in larval zebrafish (*Danio rerio*). PLoS One, 8(8), e70764. doi:10.1371/journal.pone.0070764 [PubMed: 23967101]

Larsen EH, Deaton LE, Onken H, O'Donnell M, Grosell M, Dantzler WH, and Weihrauch D (2014). Osmoregulation and excretion. Compr Physiol, 4(2), 405–573. doi:10.1002/cphy.c130004 [PubMed: 24715560]

Lignot JH, Cutler CP, Hazon N, and Cramb G (2002). Immunolocalisation of aquaporin 3 in the gill and the gastrointestinal tract of the European eel, *Anguilla anguilla* (L.). J Exp Biol, 205(Pt 17), 2653–2663. [PubMed: 12151371]

Litman T, Søgaard R, and Zeuthen T (2009). Ammonia and urea permeability of mammalian aquaporins In Beitz E (Ed.), Aquaporins (pp. 327–358): Springer.

Liu Y, Beyer A, and Aebersold R (2016). On the dependency of cellular protein levels on mRNA abundance. Cell, 165(3), 535–550. doi:10.1016/j.cell.2016.03.014 [PubMed: 27104977]

Madsen SS, Bujak J, and Tipsmark CK (2014). Aquaporin expression in the Japanese medaka (*Oryzias latipes*) in freshwater and seawater: challenging the paradigm of intestinal water transport? J Exp Biol, 217(Pt 17), 3108–3121. doi:10.1242/jeb.105098 [PubMed: 24948644]

Madsen SS, Engelund MB, and Cutler CP (2015). Water transport and functional dynamics of aquaporins in osmoregulatory organs of fishes. Biol Bull, 229(1), 70–92. doi:10.1086/BBLv229n1p70 [PubMed: 26338871]

Marshall WS and Grosell M (2006). Ion transport, osmoregulation, and acid-base balance. In The Physiology of Fishes (Vol. 3, pp. 177–230).

Marshall WS, Howard JA, Cozzi RR, and Lynch EM (2002). NaCl and fluid secretion by the intestine of the teleost *Fundulus heteroclitus*: involvement of CFTR. J Exp Biol, 205(Pt 6), 745–758. [PubMed: 11914383]

Matey V, Iftikar FI, De Boeck G, Scott GR, Sloman KA, Almeida-Val VMF, Val AL, and Wood CM (2011). Gill morphology and acute hypoxia: responses of mitochondria-rich, pavement, and mucous cells in the Amazonian oscar (Astronotus ocellatus) and the rainbow trout (*Oncorhynchus mykiss*), two species with very different approaches to the osmo-respiratory compromise. Can J Zool, 89(4), 307–324. doi:10.1139/Z11-002

Matey V, Richards JG, Wang Y, Wood CM, Rogers J, Davies R, Murray BW, Chen XQ, Du J, and Brauner CJ (2008). The effect of hypoxia on gill morphology and ionoregulatory status in the Lake Qinghai scaleless carp, *Gymnocypris przewalskii*. J Exp Biol, 211(Pt 7), 1063–1074. doi:10.1242/jeb.010181 [PubMed: 18344480]

Miller EW, Dickinson BC, and Chang CJ (2010). Aquaporin-3 mediates hydrogen peroxide uptake to regulate downstream intracellular signaling. Proc Natl Acad Sci, 107(36), 15681–15686. doi:10.1073/pnas.1005776107 [PubMed: 20724658]

Moeller HB, Olesen ET, and Fenton RA (2011). Regulation of the water channel aquaporin-2 by posttranslational modification. Am J Physiol Renal Physiol, 300(5), F1062–1073. doi:10.1152/ajprenal.00721.2010 [PubMed: 21307124]

Moorman BP, Lerner DT, Grau EG, and Seale AP (2015). The effects of acute salinity challenges on osmoregulation in Mozambique tilapia reared in a tidally changing salinity. J Exp Biol, 218(Pt 5), 731–739. doi:10.1242/jeb.112664 [PubMed: 25617466]

Nilsson S (1986). Control of gill blood flow In Nilsson S and Holmgren S (Eds.), Fish Physiology: Recent Advances (pp. 86–101). Dordrecht: Springer.

Onukwufor JO and Wood CM (2018). The osmorespiratory compromise in rainbow trout (*Oncorhynchus mykiss*): The effects of fish size, hypoxia, temperature and strenuous exercise on gill diffusive water fluxes and sodium net loss rates. Comp Biochem Physiol A Mol Integr Physiol, *219*-220, 10–18. doi:10.1016/j.cbpa.2018.02.002

Postlethwaite E and McDonald D (1995). Mechanisms of Na^+ and Cl^- regulation in freshwater-adapted rainbow trout (*Oncorhynchus mykiss*) during exercise and stress. J Exp Biol, 198(Pt 2), 295–304. [PubMed: 9317841]

Potts WTW and Fleming WR (1970). The effects of prolactin and divalent ions on the permeability to water of *Fundulus kansae*. J Exp Biol, 53(Pt 2), 317–327.

Robertson LM, Kochhann D, Bianchini A, Matey V, Almeida-Val VF, Val AL, and Wood CM (2015a). Gill paracellular permeability and the osmorespiratory compromise during exercise in the hypoxia-tolerant Amazonian oscar (*Astronotus ocellatus*). J Comp Physiol B, 185(7), 741–754. doi:10.1007/s00360-015-0918-4 [PubMed: 26115689]

Robertson LM, Val AL, Almeida-Val VF, and Wood CM (2015b). Ionoregulatory aspects of the osmorespiratory compromise during acute environmental hypoxia in 12 tropical and temperate teleosts. Physiol Biochem Zool, 88(4), 357–370. doi:10.1086/681265 [PubMed: 26052633]

Robertson LM and Wood CM (2014). Measuring gill paracellular permeability with polyethylene glycol-4000 in freely swimming trout: proof of principle. J Exp Biol, 217(Pt 9), 1425–1429. doi:10.1242/jeb.099879 [PubMed: 24436388]

Ruhr IM, Bodinier C, Mager EM, Esbaugh AJ, Williams C, Takei Y, and Grosell M (2014). Guanylin peptides regulate electrolyte and fluid transport in the Gulf toadfish (*Opsanus beta*) posterior intestine. Am J Physiol Regul Integr Comp Physiol, 307(9), R1167–1179. doi:10.1152/ajpregu.00188.2014 [PubMed: 25100079]

Ruhr IM, Schauer KL, Takei Y, and Grosell M (2018). Renoguanylin stimulates apical CFTR translocation and decreases HCO3- secretion through PKA activity in the Gulf toadfish (*Opsanus beta*). J Exp Biol, 221(Pt 6), jeb.173948. doi:10.1242/jeb.173948

Sardella BA and Brauner CJ (2007). The osmo-respiratory compromise in fish: the effects of physiological state and the environment In Fernandes MN (Ed.), Fish respiration and environment (1 ed., pp. 147–165). Boca Raton: CRC Press.

Schindelin J, Arganda-Carreras I, Frise E, Kaynig V, Longair M, Pietzsch T, Preibisch S, Rueden C, Saalfeld S, Schmid B, et al. (2012). Fiji: an open-source platform for biological-image analysis. Nat Methods, 9(7), 676–682. doi:10.1038/nmeth.2019 [PubMed: 22743772]

Scott GR, Wood CM, Sloman KA, Iftikar FI, De Boeck G, Almeida-Val VM, and Val AL (2008). Respiratory responses to progressive hypoxia in the Amazonian oscar, *Astronotus ocellatus*. Respir Physiol Neurobiol, 162(2), 109–116. doi:10.1016/j.resp.2008.05.001 [PubMed: 18555751]

Shaw JR, Sato JD, VanderHeide J, LaCasse T, Stanton CR, Lankowski A, Stanton SE, Chapline C, Coutermarsh B, Barnaby R, et al. (2008). The role of SGK and CFTR in acute adaptation to seawater in Fundulus heteroclitus. Cell Physiol Biochem, 22(1–4), 69–78. doi:10.1159/000149784 [PubMed: 18769033]

Sollid J, De Angelis P, Gundersen K, and Nilsson GE (2003). Hypoxia induces adaptive and reversible gross morphological changes in crucian carp gills. J Exp Biol, 206(Pt 20), 3667–3673. doi:10.1242/jeb.00594 [PubMed: 12966058]

Soveral G, Nielsen S, and Casini A (2018). Aquaporins in health and disease: new molecular targets for drug discovery. Boca Raton, FL, USA: CRC Press.

Stevens ED (1972). Change in body weight caused by handling and exercise in fish. J Fish Board Can, 29(2), 202–203. doi:10.1139/f72-033

Swift DJ and Lloyd R (1974). Changes in urine flow rate and haematocrit value of rainbow trout, *Salmo gairdneri* (Richardson), exposed to hypoxia. J Fish Biol, 6(4), 379–387.

Szpilbarg N and Damiano AE (2017). Expression of aquaporin-3 (AQP3) in placentas from pregnancies complicated by preeclampsia. Placenta, 59, 57–60. doi:10.1016/j.placenta.2017.09.010 [PubMed: 29108637]

Thomas S, Fievet B, and Motais R (1986). Effect of deep hypoxia on acid-base balance in trout: role of ion transfer processes. Am J Physiol Regul Integr Comp Physiol, 250(3 Pt 2), R319–327. doi:10.1152/ajpregu.1986.250.3.R319

Tingaud-Sequeira A, Calusinska M, Finn RN, Chauvigne F, Lozano J, and Cerdà J (2010). The zebrafish genome encodes the largest vertebrate repertoire of functional aquaporins with dual paralogy and substrate specificities similar to mammals. BMC Evol Biol, 10(1), 38. doi:10.1186/1471-2148-10-38 [PubMed: 20149227]

Tipsmark CK, Sørensen KJ, and Madsen SS (2010). Aquaporin expression dynamics in osmoregulatory tissues of Atlantic salmon during smoltification and seawater acclimation. J Exp Biol, 213(Pt 3), 368–379. doi:10.1242/jeb.034785 [PubMed: 20086120]

Tresguerres M, Katoh F, Fenton H, Jasinska E, and Goss GG (2005). Regulation of branchial V-H^+-ATPase, Na^+/K^+-ATPase and NHE2 in response to acid and base infusions in the Pacific spiny dogfish (*Squalus acanthias*). J Exp Biol, 208(Pt 2), 345–354. doi:10.1242/jeb.01382 [PubMed: 15634853]

Tse WKF, Au DWT, and Wong CKC (2006). Characterization of ion channel and transporter mRNA expressions in isolated gill chloride and pavement cells of seawater-acclimating eels. Biochem Biophys Res Commun, 346(4), 1181–1190. doi:10.1016/j.bbrc.2006.06.028 [PubMed: 16793006]

Verkman AS (2012). Aquaporins in clinical medicine. Annu Rev Med, 63, 303–316. doi:10.1146/annurev-med-043010-193843 [PubMed: 22248325]

Watanabe S, Kaneko T, and Aida K (2005). Aquaporin-3 expressed in the basolateral membrane of gill chloride cells in Mozambique tilapia, *Oreochromis mossambicus*, adapted to freshwater and seawater. J Exp Biol, 208(Pt 14), 2673–2682. doi:10.1242/jeb.01684 [PubMed: 16000537]

Whitehead A, Galvez F, Zhang S, Williams LM, and Oleksiak MF (2011a). Functional genomics of physiological plasticity and local adaptation in killifish. J Hered, 102(5), 499–511. doi:10.1093/jhered/esq077 [PubMed: 20581107]

Whitehead A, Roach JL, Zhang S, and Galvez F (2011b). Genomic mechanisms of evolved physiological plasticity in killifish distributed along an environmental salinity gradient. Proc Natl Acad Sci, 108(15), 6193–6198. doi:10.1073/pnas.1017542108 [PubMed: 21444822]

Wood CM (1988). Acid-base and ionic exchanges at gills and kidney after exhaustive exercise in the rainbow trout. J Exp Biol, 136(Pt 1), 461–481.

Wood CM, Bucking C, and Grosell M (2010). Acid-base responses to feeding and intestinal Cl^- uptake in freshwater- and seawater-acclimated killifish, *Fundulus heteroclitus*, an agastric euryhaline teleost. J Exp Biol, 213(Pt 15), 2681–2692. doi:10.1242/jeb.039164 [PubMed: 20639430]

Wood CM and Grosell M (2008). A critical analysis of transepithelial potential in intact killifish (*Fundulus heteroclitus*) subjected to acute and chronic changes in salinity. J Comp Physiol B, 178(6), 713–727. doi:10.1007/s00360-008-0260-1 [PubMed: 18379791]

Wood CM and Grosell M (2012). Independence of net water flux from paracellular permeability in the intestine of *Fundulus heteroclitus*, a euryhaline teleost. J Exp Biol, 215(Pt 3), 508–517. doi:10.1242/jeb.060004 [PubMed: 22246259]

Wood CM, Iftikar FI, Scott GR, De Boeck G, Sloman KA, Matey V, Valdez Domingos FX, Duarte RM, Almeida-Val VM, and Val AL (2009). Regulation of gill transcellular permeability and renal function during acute hypoxia in the Amazonian oscar (*Astronotus ocellatus*): new angles to the osmorespiratory compromise. J Exp Biol, 212(Pt 12), 1949–1964. doi:10.1242/jeb.028464 [PubMed: 19483013]

Wood CM, Kajimura M, Sloman KA, Scott GR, Walsh PJ, Almeida-Val VM, and Val AL (2007). Rapid regulation of Na^+ fluxes and ammonia excretion in response to acute environmental hypoxia in the Amazonian oscar, *Astronotus ocellatus*. Am J Physiol Regul Integr Comp Physiol, 292(5), R2048–2058. doi:10.1152/ajpregu.00640.2006 [PubMed: 17272664]

Wood CM and Randall DJ (1973a). The influence of swimming activity on water balance in the rainbow trout (*Salmo gairdneri*). J Comp Physiol, 82(3), 257–276.

Wood CM and Randall DJ (1973b). Sodium balance in the rainbow trout (*Salmo gairdneri*) during extended exercise. J Comp Physiol B, 82(3), 235–256.

Wood CM, Ruhr IM, Schauer KL, Wang Y, Mager EM, McDonald MD, Stanton B, and Grosell M (2019). The osmorespiratory compromise in the euryhaline killifish: water regulation during hypoxia. J Exp Biol, jeb.204818. doi:10.1242/jeb.204818

Yamamoto N, Yoneda K, Asai K, Sobue K, Tada T, Fujita Y, Katsuya H, Fujita M, Aihara N, Mase M, et al. (2001). Alterations in the expression of the AQP family in cultured rat astrocytes during hypoxia and reoxygenation. Brain Res Mol Brain Res, 90(1), 26–38. doi:10.1016/s0169-328x(01)00064-x [PubMed: 11376853]

Zhao S and Fernald RD (2005). Comprehensive algorithm for quantitative real-time polymerase chain reaction. J Comput Biol, 12(8), 1047–1064. doi:10.1089/cmb.2005.12.1047 [PubMed: 16241897]

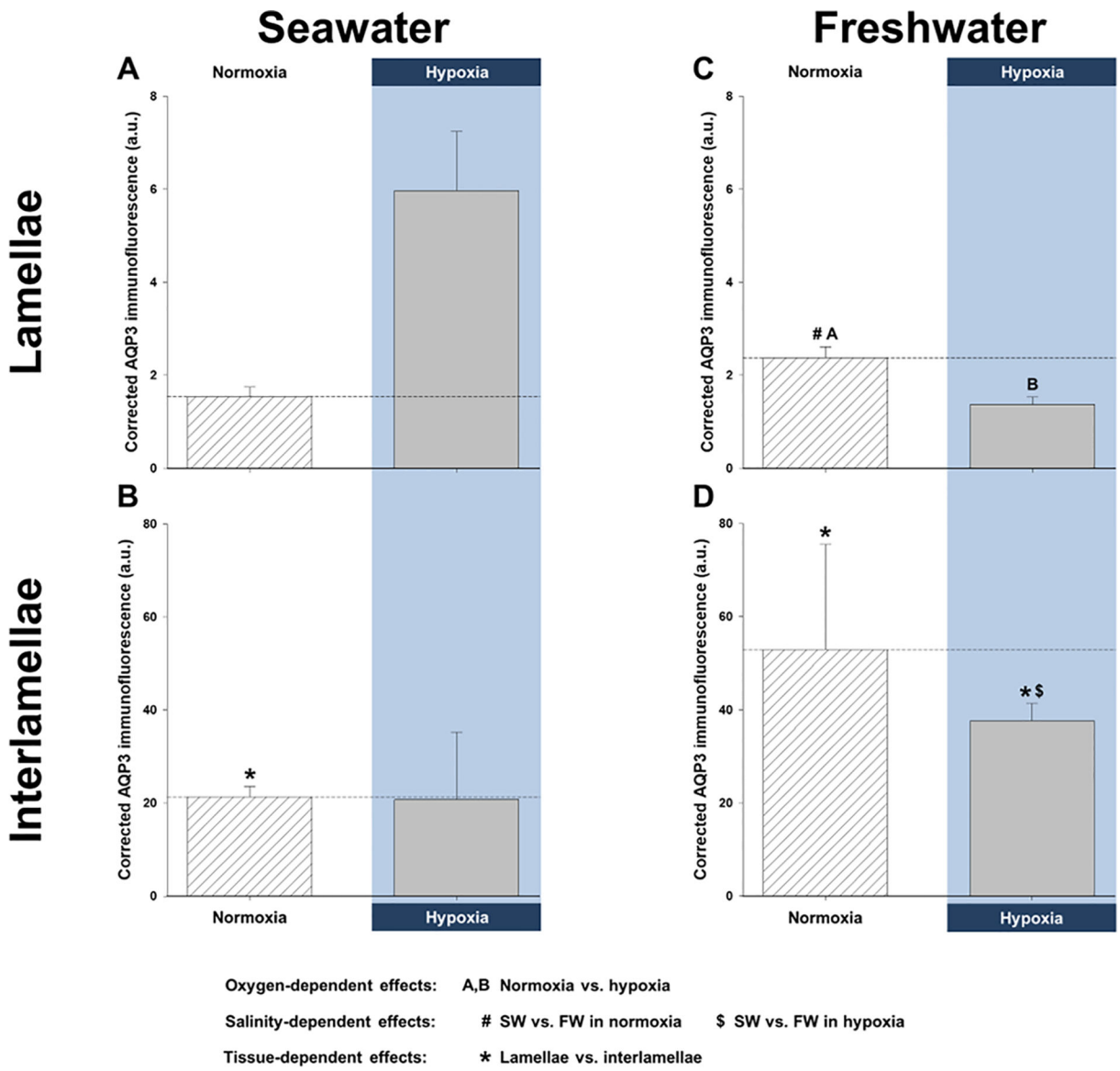

Figure 1. Effects of salinity and dissolved oxygen on branchial protein abundance of killifish aquaporin-3 (AQP3).

Killifish were acclimated to either seawater or freshwater, and subjected to normoxia (the control), 3 h hypoxia (10% O_2 saturation), or normoxic recovery, after which the gills were excised. Three fractions were isolated from the gills (whole cell, cytoplasm, and cell membrane) and western blots were run to determine AQP3 protein abundance. (A) Whole-cell, (B) cytoplasmic, and (C) cell-membrane gill fractions of seawater-acclimated fish. (D) Whole-cell, (E) cytoplasmic, and (F) cell-membrane fractions of freshwater-acclimated fish. Data were normalized to normoxic protein levels and are shown as means ± SEM (N = 4–5). Significant differences in AQP3 protein abundance between normoxia, hypoxia, and recovery are indicated for oxygen-dependent effects, by dissimilar upper-case letters (A, B), when $P \leq 0.05$. Note that seawater and freshwater samples were run on different gels, so cannot be compared statistically.

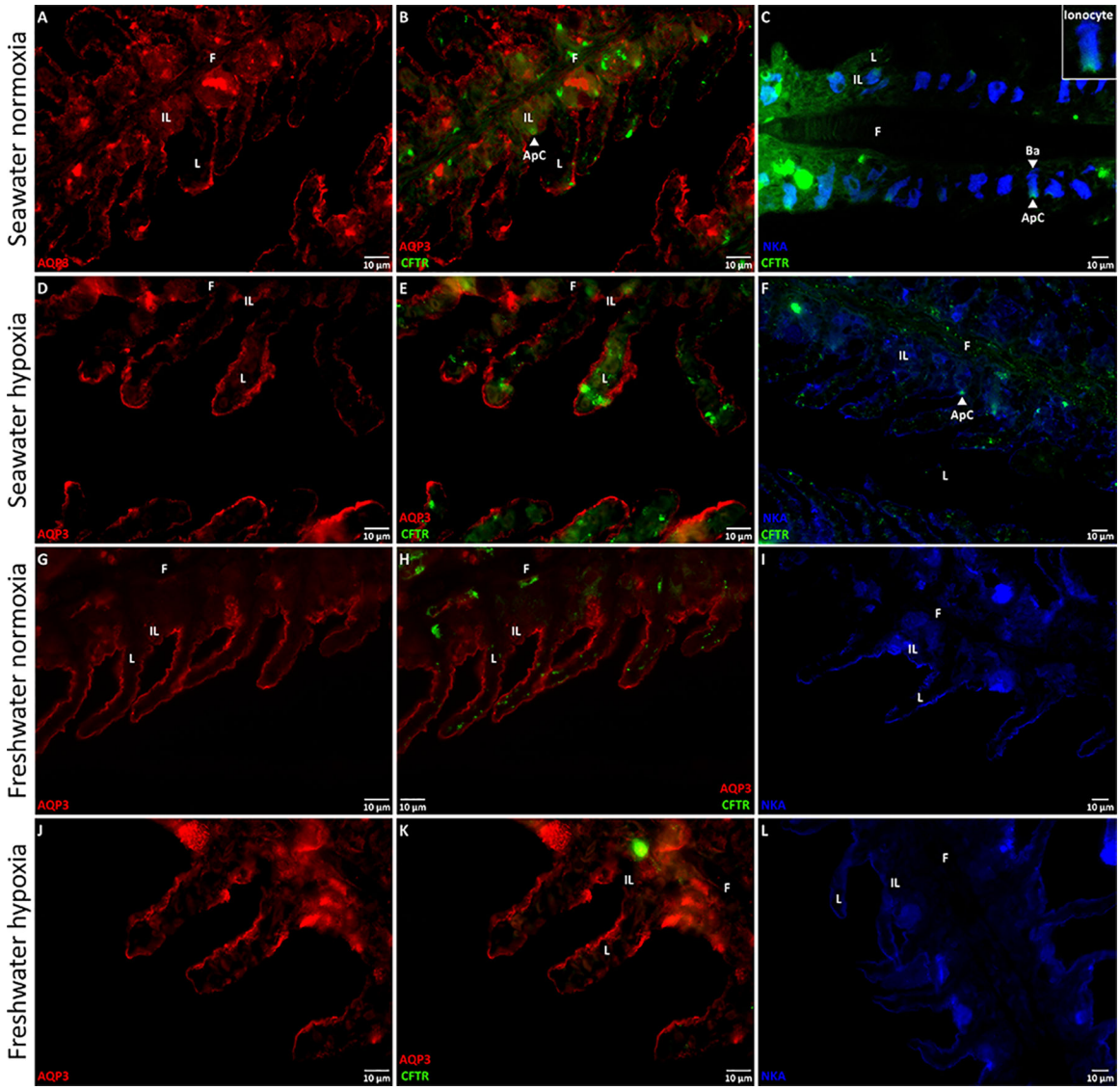

Figure 2. Effects of salinity and dissolved oxygen on branchial and intestinal mRNA expression of killifish aquaporin-3 (AQP3).

Killifish were acclimated to either seawater or freshwater, and subjected to normoxia (the control) or 3 h hypoxia (10% O_2 saturation), after which the gills and intestine were excised. Relative AQP3 mRNA expression was determined by real-time, quantitative PCR and normalized by calibrating with EF1α. mRNA expression in (A) seawater and (B) freshwater of the gills and in (C) seawater and (D) freshwater of the intestine. Data are shown as means ± SEM (N = 6 fish per treatment). Significant differences in AQP3 mRNA expression are indicated for oxygen-dependent effects, by dissimilar upper-case letters (A, B), and for salinity-dependent effects, by pound signs (#) and dollar symbols ($), when $P \leq 0.05$, as shown in the figure legend (tissue-dependent effects were not analyzed). Although not indicated, freshwater resulted in significantly higher total branchial AQP3 mRNA expression.

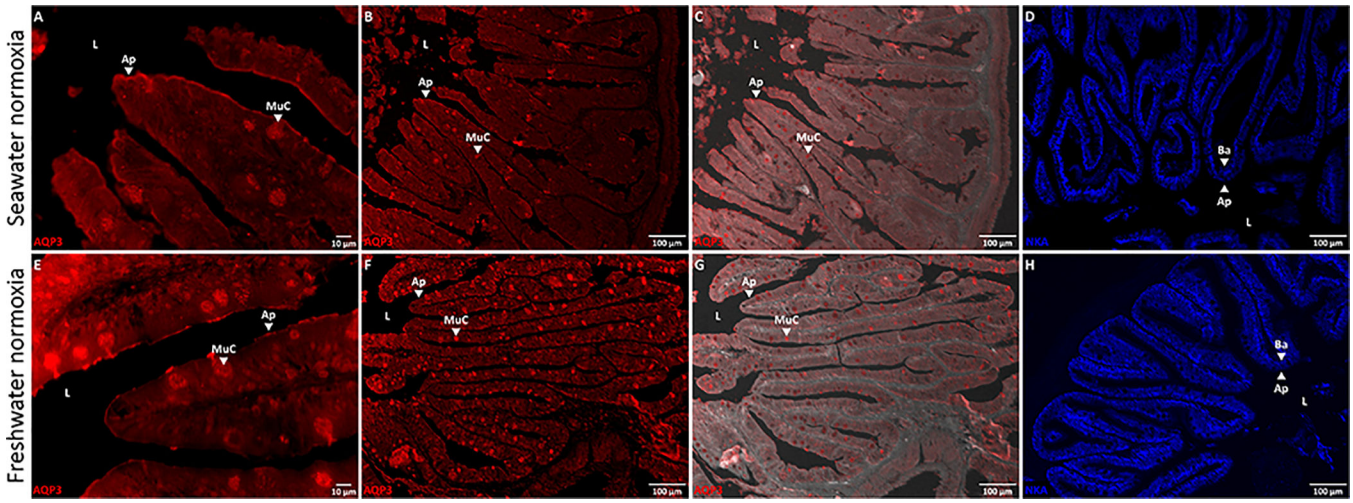

Figure 3. Effects of salinity and dissolved oxygen on killifish aquaporin-3 (AQP3) protein immunofluorescence in the lamellae and interlamellae of the gills.

Killifish were acclimated to either seawater or freshwater, and subjected to normoxia (the control) or 3 h hypoxia (10% O_2 saturation), after which the gills were excised. Relative corrected AQP3 immunofluorescence [in arbitrary units (a.u.)] measured in the (A) lamellae and (B) interlamellae of seawater-acclimated fish and in the (C) lamellae and (D) interlamellae of freshwater-acclimated fish. Note the difference in scale between Panels A and C (lamellae) versus B and D (interlamellae), demonstrating that the majority of AQP3 immunofluorescence is in the interlamellar regions of the gill. Data are shown as means ± SEM (N = 6 different fish per treatment). Significant differences in AQP3 immunofluorescence are indicated for oxygen-dependent effects, by dissimilar upper-case letters (A, B), for salinity-dependent effects, by pound signs (#) and dollar symbols ($), and for tissue-dependent effects, by asterisks (*), when $P \leq 0.05$, as shown in the figure legend. Although not indicated, freshwater resulted in significantly higher total branchial AQP3 immunofluorescence than in seawater, and total AQP3 immunofluorescence was significantly lower in hypoxic vs. normoxic freshwater.

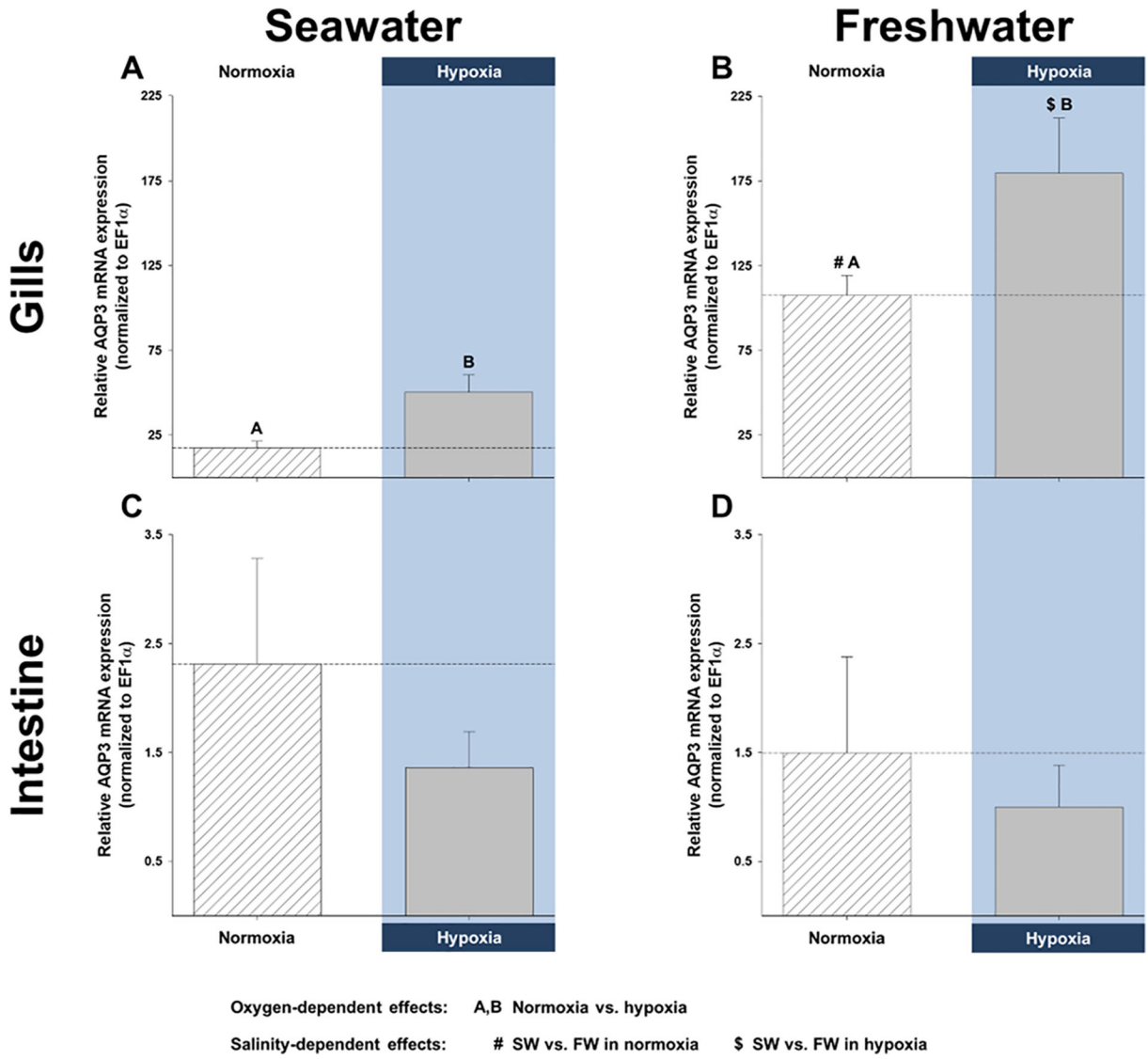

Figure 4. Representative immunofluorescent images of aquaporin-3 (AQP3), the cystic fibrosis transmembrane conductance regulator (CFTR), and the Na^+/K^+-ATPase (NKA) in killifish gills.

Killifish were acclimated to either seawater or freshwater, and subjected to normoxia (the control) or 3 h hypoxia (10% O_2 saturation), after which the gills were excised. Immunohistochemistry was used to identify the membrane localization of AQP3 (in red), CFTR (in green), and NKA (in blue), with immunofluorescent antibodies, in seawater normoxia (A, B, and C) or hypoxia (D, E, and F) and in freshwater normoxia (G, H, and I) or hypoxia (J, K, and L). All immunofluorescent images of AQP3/CFTR are in 60x and those of NKA are in 40x. AQP3 immunofluorescence generally shared the same distribution as NKA; AQP3 was localized to the basolateral membranes (Ba; example shown on Panel C) of the cells of both the gill lamellae (L), and interlamellar regions (IL) of the filaments (F). AQP3 might also occur on the apical membranes at the outer borders of the lamellae. CFTR immunofluorescence was poor in the freshwater gills, but was clearly discernible in the apical membrane of the interlamellae of seawater gills. NKA immunofluorescence was expressed on the basolateral membranes of the cells of the lamella and interlamellae under

all treatments, and was particularly prominent in the interlamellar regions of the seawater gill under normoxia. Ionocytes (inset on Panel C) were apparent in the interlamellar regions of seawater gills under normoxia and hypoxia and were distinguishable by an apical crypt (ApC; Panels C and F) expressing CFTR and the basolateral membrane expressing NKA.

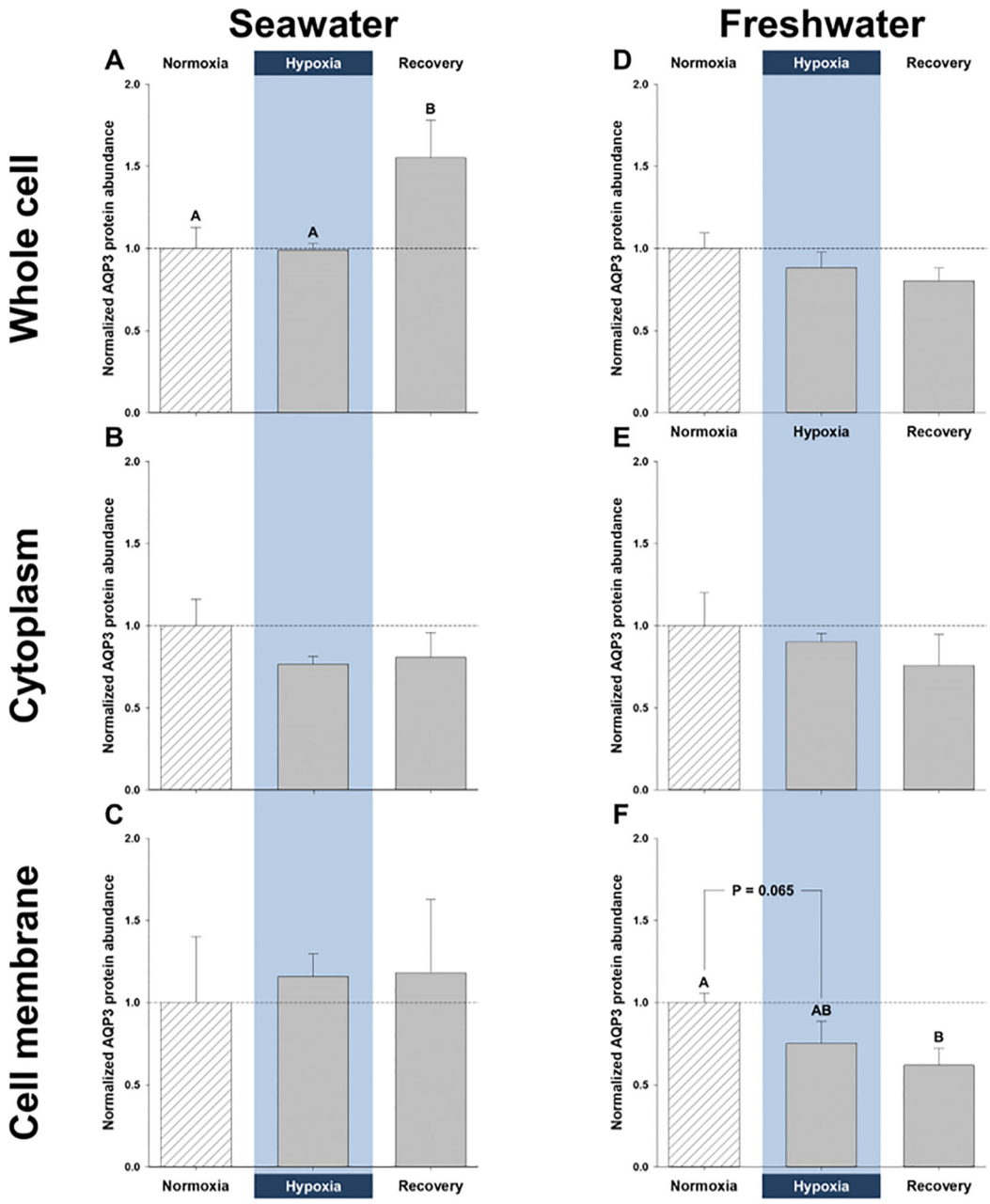

Figure 5. Immunofluorescent images of aquaporin-3 (AQP3) and the Na^+/K^+-ATPase (NKA) in the killifish intestine.

Killifish were acclimated to either seawater or freshwater and immunohistochemistry was used to identify the membrane localization of AQP3 (in red) and NKA (in blue), with immunofluorescent antibodies. (A and E) 60x, (B and F) 10x, and (C and G) 10x brightfield-overlaid images of AQP3 immunofluorescence in the killifish intestine. (D and H) 10x images of NKA immunofluorescence in the killifish intestine. AQP3 immunofluorescence is localized to the apical membrane (Ap) and mucus cells (MuC) of the enterocytes – facing the intestinal lumen (L) – and is distributed differently than NKA immunofluorescence, which is exclusively basolateral (Ba).